


## Article

# Eco-Friendly Fire-Resistant Coatings Containing Dihydrogen Ammonium Phosphate Microcapsules and Tannins

Andrés Felipe Jaramillo <sup>1,\*</sup> , Andrés Díaz-Gómez <sup>2</sup>, Jesús Ramirez <sup>2</sup>, María Elizabeth Berrio <sup>2</sup>, Vanessa Cornejo <sup>2</sup>, David Rojas <sup>2</sup>, Luis Felipe Montoya <sup>2</sup>, Adriana Mera <sup>3</sup> and Manuel Francisco Melendrez <sup>2,4,\*</sup>

<sup>1</sup> Department of Mechanical Engineering, Universidad de La Frontera, 01145 Francisco Salazar, Temuco 4780000, Chile

<sup>2</sup> Interdisciplinary Group of Applied Nanotechnology (GINA), Hybrid Materials Laboratory (HML), Department of Materials Engineering (DIMAT), Faculty of Engineering, University of Concepcion, 270 Edmundo Larenas, Box 160-C, Concepcion 4070409, Chile; andresdiaz.qind@gmail.com (A.D.-G.); alframirez09@gmail.com (J.R.); maelibeni2018@gmail.com (M.E.B.); vanecornejo@udec.cl (V.C.); davrojas@udec.cl (D.R.); luismontoya@udec.cl (L.F.M.)

<sup>3</sup> Instituto de Investigación Multidisciplinario en Ciencia y Tecnología, Universidad de La Serena, Benavente 980, La Serena 1700000, Chile; amera@userena.cl

<sup>4</sup> Unidad de Desarrollo Tecnológico, 2634 Av. Cordillera, Parque Industrial Coronel, Box 4051, Concepción 4191996, Chile

\* Correspondence: andresfelipe.jaramillo@ufrontera.cl (A.F.J.); mmelendrez@udec.cl (M.F.M.); Tel.: +56-45-2325981 (A.F.J.); +56-41-2203187 (M.F.M.)



**Citation:** Jaramillo, A.F.; Díaz-Gómez, A.; Ramirez, J.; Berrio, M.E.; Cornejo, V.; Rojas, D.; Montoya, L.F.; Mera, A.; Melendrez, M.F. Eco-Friendly Fire-Resistant Coatings Containing Dihydrogen Ammonium Phosphate Microcapsules and Tannins. *Coatings* **2021**, *11*, 280. <https://doi.org/10.3390/coatings11030280>

Received: 25 January 2021

Accepted: 24 February 2021

Published: 27 February 2021

**Publisher's Note:** MDPI stays neutral with regard to jurisdictional claims in published maps and institutional affiliations.



**Copyright:** © 2021 by the authors. Licensee MDPI, Basel, Switzerland. This article is an open access article distributed under the terms and conditions of the Creative Commons Attribution (CC BY) license (<https://creativecommons.org/licenses/by/4.0/>).

**Abstract:** The effect of microencapsulation of dihydrogen ammonium phosphate (MAP) in the generation of fire-resistant coatings was studied in the presence of tannins extracted from *Pinus radiata*. MAP was encapsulated to avoid interaction with sodium carbonate ( $\text{Na}_2\text{CO}_3$ ), which, upon contact with fire, generates unwanted gases. Thus, a fireproof (or intumescent) protective film was produced in the presence of the tannins. Microcapsules were polymerized with melamine and characterized by Fourier Transform Infrared Spectroscopy (FTIR), Thermogravimetric Analysis (TGA), and scanning electron microscopy (SEM)-Energy-Dispersive X-ray Spectroscopy (EDS). The microcapsules were spherical with diameters between 0.7 and 1  $\mu\text{m}$ . The as-produced microcapsules were mixed with tannin extract and the properties of their films were evaluated on wood and structural steel substrates; their fire resistance on medium density fiberboard was also evaluated. Flame resistance tests showed a carbonization index of 26.86% using microcapsules (3% *w/w*); this is better than commercial coatings. The film properties were similar to commercial coatings, but the adherence was slightly decreased due to agglomeration and also film flexibility.

**Keywords:** fire resistant coating; tannin; eco-friendly; microencapsulation; dihydrogen ammonium phosphate

## 1. Introduction

Structural steel has been widely used in the construction industry due to properties such as high strength/weight ratio, high ductility, among others. However, its mechanical resistance decreases if the temperature exceeds 500 °C during a fire. Therefore, enhancing this property is a concern for the construction industry; additionally, technological solutions focused mainly on the development of foams and coatings have been proposed [1]. Fire-resistant coatings (fire retardant and intumescent) have been widely used to protect metal structures and even wood substrates. These types of fire-resistant coatings are composed of a carbon forming material, a mineral acid catalyst, a blowing agent, and a binder resin. During the combustion process, these components operate synergistically to form a honeycomb carbon structure that thermally isolates the coated steel substrate and establishes a protective barrier blocking heat transfer to the steel; while in wood, it acts

chemically to release less pyrolysis gasses and contains more of the fuel as thermally insulating char [2,3]. The mechanism of protection in fireproof coatings includes retarding the advance of flames on the substrate. On the other hand, in intumescent coatings, the acidic source can release  $\text{NH}_3$  and organic acids during the combustion process; this initiates an esterification reaction with the carbonaceous agent. The carbonaceous agent is carbonized by dehydration, and finally, the blowing agent forms an intumescent foam or layer on the surface of the polymeric material [1,4]. These coatings have numerous disadvantages: the carbon protective layer is vulnerable to high temperatures, the coating is prone to aging, and in water-based coatings, the coating displays poor adhesion to substrates [5,6].

To achieve suitable fire resistance, coatings are generally formulated with a high content of solid fillers; these impair the mechanical properties and durability of the film. Moreover, a major disadvantage of additives is their poor compatibility with the coating resin; this significantly reduces the protection capacity in a fire. There has been limited use of microencapsulation technology in fire retardants and intumescent coatings. Almost no research has been conducted on the durability and fire resistance of the flame-retardant coating after the static immersion test. To overcome these problems, the use of microencapsulated dihydrogen ammonium or monoammonium phosphate (MAP) (acid source) as a fire-resistant additive has been an effective strategy [7,8].

For the scientific and industry communities, the development of ecological and sustainable fire-resistant coating systems has become an urgent challenge. Recently, the study of products from natural sources as potential additives has garnered considerable attention. Their characteristics allow the generation of an insulating carbon layer on substrate surfaces. They provide efficient fire resistance functionality and are therefore promising alternatives to halogen-based chemicals. Almost all renewable resource-based additive approaches to form fire-resistant coatings can impart these beneficial properties [9,10]. Modifying the additive properties through microencapsulation with water or insoluble polymers is an effective method to improve water resistance and polarity. Wu et al. [11] studied flame retardation in microencapsulated ammonium polyphosphate and demonstrated a decrease in particle size upon encapsulation and low water absorption. This result is of great interest since the particle size influences the mechanical properties of the coatings. To solve the aforementioned problems, and to investigate lower toxicity coatings, the microencapsulation of dihydrogen phosphate (MAP) as an acid source and low molecular weight tannins as a carbonaceous agent is proposed.

Tannins extracted from *Pinus radiata* are mixtures of simple phenols such as gallic acid and sugar esters (primarily glucose and gallic/digallic acids). The presence of gallic acid in hydrolyzable tannins makes them ideal raw materials for preparing the coatings [12,13]. Likewise, the presence of hydroxyl groups in tannins, together with their high reactivity compared to resorcinol and phenol, make them ideal candidates to produce fire-resistant coatings [14]. Tannins have been used in the production of rigid foams, presenting similar fire-retardant properties to formulations that incorporate specialized additives such as boric acid ( $\text{H}_3\text{BO}_3$ ) or phosphoric acid ( $\text{H}_3\text{PO}_4$ ). Tannins are obtained from waste bark making them a renewable material, and, once extracted, the bark does not lose its calorific capacity and can be used in industrial boilers.

With increasing focus on sustainability in the construction industry, multistory timber buildings are becoming increasingly popular. The fire issue becomes important since both the wooden claddings and the building construction itself may be involved in the combustion. In this study, the effect of MAP microencapsulation for the generation of a fire-resistant coating, in the presence of tannins (extracted from *Pinus radiata* as a carbon source), was examined [15]. The mechanical properties of the obtained coatings were compared and their fire resistance was evaluated. The fire-retardant properties of the coatings were evaluated according to ASTM D1360-90a [16] standard methods; this allowed for an indication of the carbonization index and the weight loss of the substrate. The morphologies of the microcapsules were revealed by scanning electron microscopy (SEM) and the changes in the chemical structure were recorded using Fourier Transform

Infrared Spectroscopy (FTIR). The mechanical film properties were determined using ISO and ASTM standard methodologies.

## 2. Materials and Methods

The reagents used for the microencapsulation of dihydrogen ammonium phosphate or monoammonium phosphate (MAP) were as follows: 2,4,6-triamine-1,3,5-triazine (melamine), polyvinyl alcohol (PVA), ethanol (96% *v/v*), monoammonium phosphate (MAP), formaldehyde (37% *v/v*), sodium carbonate ( $\text{Na}_2\text{CO}_3$ ), and acetic acid. These were analytical grade and supplied by Merck SA. Pinus radiata tannins were extracted according to the procedure described by Bacalandro et al. [17] and were used as a carbon source. The bark of Pinus radiata was added to a pilot reactor, and extraction with a mixture of ethanol/water was performed under reduced pressure. The extract was subsequently dried in an oven at 40 °C under reduced pressure until a fine tannin powder was obtained. The appropriate amount of tannin extract or low molecular weight tannins (L-MWT) was dissolved in water to make up the fractions used in this study.

### 2.1. Synthesis of the Prepolymer and Preparation of the MAP Microcapsules

The prepolymer was synthesized using a modified version of the method reported by Wu et al. [11]. In total, 2 g of PVA and 2 g of melanin were added to a 500 mL round bottom flask, followed by 100 mL of distilled water. After the dissolution of the solids, the pH of the solution was adjusted to 4–5 using acetic acid and was then heated at 90 °C in an oil bath for 1.5 h with constant stirring. Subsequently, the pH of the solution was adjusted to between 8 and 9 using a 10% (*w/v*)  $\text{Na}_2\text{CO}_3$  solution, and another 2 g of melanin was added first, followed by the 5 mL of formaldehyde 37% (*v/v*). Finally, the obtained mixture was heated at 90 °C for 1 h to obtain the prepolymer. MAP microcapsules were prepared as follows: 10 g of MAP was dispersed in 25 mL of ethanol by stirring at 1000 rpm for 5 min. Afterward, this solution was added to the prepolymer obtained previously and the pH of the mixture was adjusted to between 4 and 5 using a 10% (*v/v*)  $\text{H}_2\text{SO}_4$  solution. The resultant solution was heated to 80 °C with constant stirring at 400 rpm for 3 h. The solution was then centrifuged at 9000 rpm for 15 min. The obtained microcapsules were filtered and washed with distilled water and dried in an oven at 70 °C for 24 h. The obtained solid was denoted as microcapsules of monoammonium phosphate (McMAP).

### 2.2. Coating Formulation, Surface Preparation, and Application onto Substrates

Three coatings were produced, each with a different formulation, to determine the effect of the incorporation of microcapsules in active additives on the fire resistance. A water-based acrylic coating was created as a control sample. Microcapsules of MAP (McMAPs) were added to this coating at 3% and 9% *w/w* ratios. The coatings were formulated with  $\lambda$  values between 1.37 and 1.51, where  $\lambda$  is the relationship between the pigment volume concentrations (PVC) (50% to 65%) and the critical pigment volume concentration (CPVCs) (36% to 43%) [18,19]. Table 1 shows the compositions of the coating components. The preparation of the coatings was achieved with a mechanical stirrer and a Cowles-type dispersion propeller operated at speeds of 550–700 rpm. The components were added into a 1 L plastic container and were constantly agitated by varying the speed of the rotor. Zirconia grinding balls were used to ensure adequate dispersion and to reduce the particle size to a value of 5 Hegman (35–40  $\mu\text{m}$ ). The surfaces of the metal substrates (Steel ASTM A36) were prepared according to the established standards of the Steel Structures Painting Council (SSPC; Pittsburgh, PA, USA), applying section SP1 (Solvent Cleaning: removal of all visible oil, grease, soil, drawing and cutting compounds, and other soluble contaminants from steel surfaces with solvent, vapor, cleaning compound, alkali, emulsifying agent, or steam) and SP5 (Metal blast cleaning: when viewed without magnification, the surface shall be free of all visible oil, grease, dust, dirt, mill scale, rust, coating, oxides, corrosion products, and other foreign matter).

**Table 1.** Specifications of the experimental materials in the blank formulations F3, and F9. All formulations were prepared in (*w/w*)—3 and 9 indicate the percentage of microcapsules of monoammonium phosphate (McMAPs) used.

Formulations	F-Blank	F-3% McMAP	F-9% McMAP
Components			
Water	27.80	27.74	27.80
Caolín (Opacit)	5.12	4.75	4.75
Calcium carbonate (Hifill)	13.33	12.35	3.01
L-MWT	15.50	15.00	15.00
McMAP	0.00	3.01	9.03
Foamaster MO 2134	0.16	0.14	0.14
Acronal S716 1.09	31.00	26.00	26.00

The wood substrate was dried in an oven at 30 °C for 48 h and the adhered powders were superficially cleaned. Due to their high solid content, the formulated coatings were applied onto the substrates using a brush. The thickness of the films was between 150 and 200 µm. The formulated coatings were denoted as: F-Blank (acrylic water-based formulation); F-3% McMAPs (parent formulation + 3% *w/w* McMAP); and F-9% McMAPs (blank + 9% *w/w* McMAP). In addition, two commercial coatings were tested for comparison; intumescent FireWall 200 commercial paint (C-INT) (Tricolor, Santiago, Chile) and Retardant 77 commercial paint (C-IGN) (Chilcorrofin, Santiago, Chile).

### 2.3. Characterization and Fire Behavior Tests

#### 2.3.1. Chemical, Morphological, and Structural Characterization of Microcapsules

The obtained microcapsules were characterized by Attenuated Total Reflection Fourier Transform Infrared Spectroscopy (ATR-FTIR) using a Spectrum Two kit (Perkin Elmer, Waltham, MA, USA). Each spectrum was obtained by consecutive scanning at a resolution of 1 cm<sup>−1</sup> over the range 4000–500 cm<sup>−1</sup>. The morphological characteristics of the microcapsules were revealed by Scanning Electron Microscopy (SEM) using a Jeol JSM 6380 LY (JEOL, Tokyo, Japan) operated at an acceleration voltage of 20 kV. Before SEM analysis, the samples were coated with 50 nm of gold. Elements present in the microcapsule were qualitatively determined by Energy-Dispersive X-ray Spectroscopy (EDS).

#### 2.3.2. Thermogravimetric Analysis (TGA)

TGA was performed using a Pyris TGA kit (TG 209 F3 Tarsus, Waltham, MA, USA). Further, 5 mg of the microcapsules was placed in an aluminum crucible and subjected to a heating cycle over the range 25–600 °C. The heating rate was 10 °C/min. The system was purged with nitrogen at a flow rate of 50 mL/min.

#### 2.3.3. Evaluation of the Properties of the Coatings

A range of mechanical assessments were conducted on the coated substrates and the commercial coatings according to standard ASTM and ISO testing methodologies. The dynamic viscosity of the coating was measured using a Krebs viscometer (FLSmidth, Copenhagen, Denmark) in accordance with ASTM D562 [20], while the dry film thickness was measured according to ASTM D6132 [21] using an Elcometer 456 kit (Elcometer, Warren, MI, USA). To determine the hydrophobicity of the coating, the contact angle (CA) formed between the coating and a drop of deionized water was determined. The change of the angle over numerous periods of 10 s, in static conditions, was evaluated with a Kruss Goniometer model DSA25S (Kruss Scientific, Hamburg, Germany) controlled by software. The average CA value was obtained by measuring the same sample in different positions.

Mechanical properties were evaluated on metallic substrates with dimensions of  $10 \times 10 \times 0.3 \text{ cm}^3$  for cupping, adhesion, and abrasion tests. Flexibility tests were completed on substrates with dimensions of  $15 \times 6 \times 0.3 \text{ cm}^3$ . The standards applied for these tests were as follows: adherence (ASTM D4541 [22] using a PosiTest AT-A kit (DeFelsko Corporation, Ogdensburg, NY, USA)), abrasion (ASTM D4060 [23] using a Taber Abraser model 5135 kit with a load of 1000 kg and type CS-10 abrasion wheels), flexibility (ISO 1519 [24] using a BYK cylinder mandrel 5710 (BYK-Instrument, Pompano Beach, FL, USA)), and cupping (ISO 1520 [25] using a BYK PF-5405 cupping machine (BYK-Instrument, Pompano Beach, FL, USA)).

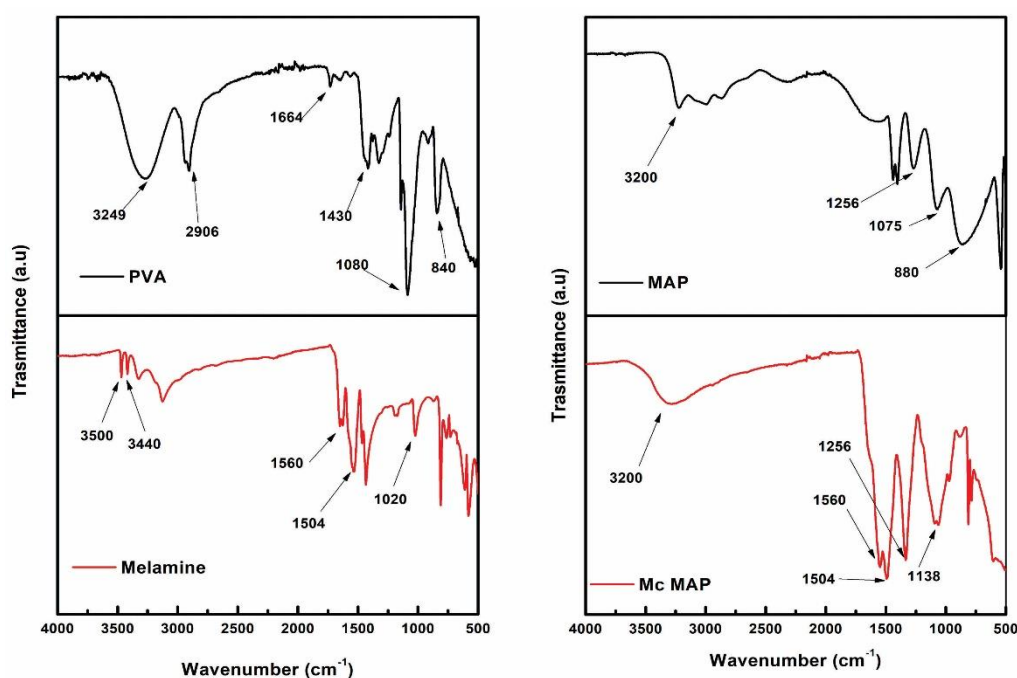
### 2.3.4. Fire Behavior of the Coating

The fire resistance of the coatings was evaluated using an adapted version of ASTM D1360-90a. A constant flame was applied by a torch, at an inclination of  $45^\circ$  to the sample, for 180 s, taking temperature measurements of the area every 15 s. The tests were carried out in triplicates for each formulation. In addition, the weight, width, length, and initial and final thickness of each specimen were recorded throughout the test. Thus, the carbonization index, weight loss, and resistance to temperature increases were evaluated.

## 3. Results and Discussions

### 3.1. Chemical, Morphological, and Structural Characterization of Microcapsules

The FTIR spectra of the encapsulating materials (melamine and PVA) are shown in Figure 1a, while the spectra of the additive to be encapsulated (MAP) and the obtained microcapsules (McMAPs) are presented in Figure 1b. Table 2 summarizes the characteristic vibrational bonding signals of the samples. Based on these results, the formation of the McMAPs is evidenced by the disappearance of the stretching bands of the primary amine from the melamine ( $3500$  and  $3440 \text{ cm}^{-1}$ ). This indicates that the reaction with polyvinyl alcohol to form the prepolymer was successful. The appearance of the vinylidene stretching signal at  $1664 \text{ cm}^{-1}$  originating from the PVA, as well as the characteristic stretching signal at  $3200 \text{ cm}^{-1}$  related to alcohol groups that did not react, confirm the formation of the encapsulating polymer. The encapsulated MAP signals observed at  $1256$  and  $880 \text{ cm}^{-1}$  are ascribed to  $\text{P}=\text{O}$  stretching and  $\text{P}-\text{O}$  asymmetric stretching vibrations, respectively [11,26].

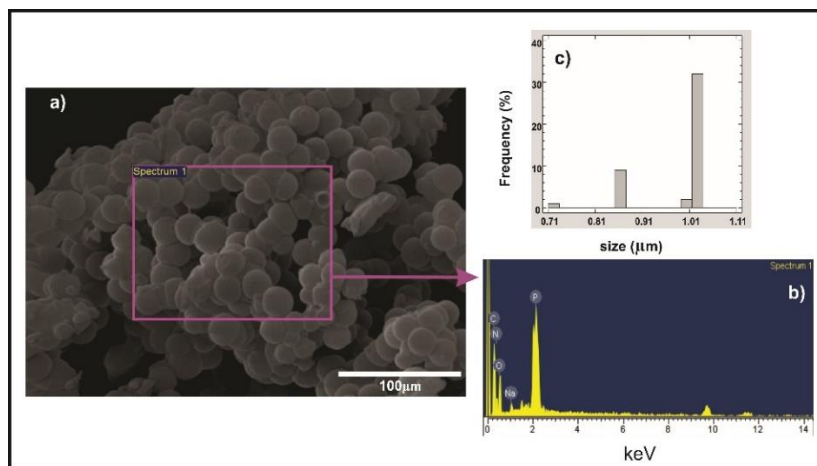


**Figure 1.** Fourier Transform Infrared Spectroscopy (FTIR) spectra of the microencapsulation of dihydrogen ammonium phosphate (MAP) materials.

**Table 2.** Infrared vibration signals from reagents and microcapsules.

Vibration Signal	Melamine	PVA	MAP	McMAP
	Wavenumber ( $\text{cm}^{-1}$ )			
N–H Stretching Primary Amine	3500 3440	–	–	–
N=C Stretching	1630	–	–	–
N–H Bending Primary Amine	1560	–	–	1560
N–C Stretching	1020	–	–	1138
O–H Stretching Alcohol	–	3249	–	3200
C–H Stretching $\text{sp}^2$ $\text{sp}^3$	–	2936 2906	–	–
C=C Stretching alkene	–	1664	–	1664
C–H Bending alkane	–	1430	–	–
O–H Bending	–	1330	–	–
C=C Bending alkene	–	840	–	–
$\text{NH}_4^+$	–	–	3200	–
P=O Stretching	–	–	1256	1256
P–O Symmetric Stretching	–	–	1075	–
P–O Asymmetric Stretching	–	–	880	880

Figure 2 shows the surface morphology, particle diameter, and EDS analysis of the McMAPs. Perfectly spherical microcapsules were observed with uniform size and no irregularities. The particle size distribution varied between 0.7 and 1  $\mu\text{m}$  with an average diameter of 0.98  $\mu\text{m}$  (Figure 2a,c). The diameters of the obtained microcapsules were smaller than those reported by Wu et al. [11] (20  $\mu\text{m}$ ). Furthermore, compositional analysis by EDS (Figure 2b) showed characteristic signals for C, N, P, and O; these results confirm the MAP encapsulation. The compositional mapping of the McMAPs is illustrated in Figure 3; a homogeneous distribution of each element was seen throughout the microcapsule. The presence of carbon is attributed to the fact that the microcapsule is an organic polymer formed from PVA, melamine, and formaldehyde. The presence of nitrogen results from the incorporation of melamine in the polymer matrix while the observed phosphorus signal is due to monoammonium phosphate existing both inside the microcapsule and in its wall.

**Figure 2.** (a) Scanning electron microscopy (SEM) micrographs of the McMAPs and (b) size distribution histogram for the microcapsules. (c) Energy-dispersive X-ray spectrometry (EDS) analysis.

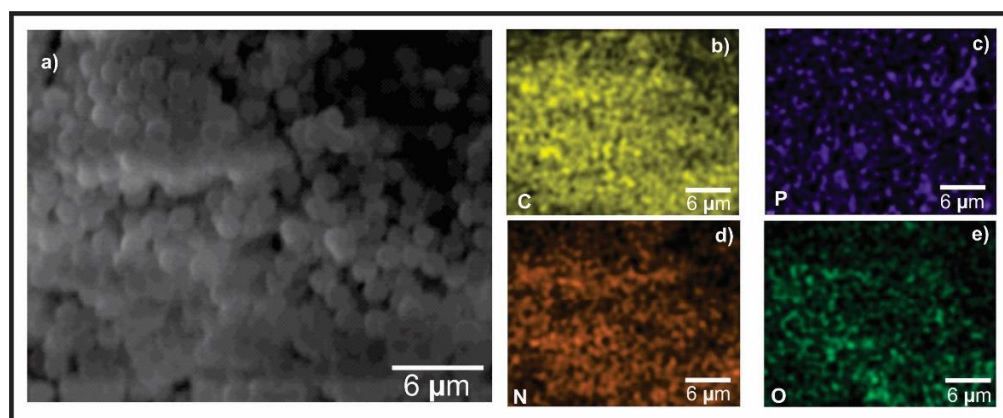


**Figure 3.** (a) McMAP EDS mapping image and distributions of the various elements that make up the microcapsules: (b) carbon (C), (c) phosphorus (P), (d) nitrogen (N), and (e) oxygen (O).

### 3.2. Thermogravimetric Analysis (TGA)

The thermogravimetric analysis (TGA) curve and Differential Thermogravimetric Analysis (DTG) for the McMAPs are shown in Figure 4 and the decomposition temperatures are reported in Table 3. Only 26.51% of the initial mass was retained at 600 °C as revealed in the TGA curve. The observed loss of mass corresponds to the thermal degradation of the microcapsules. Upon determining the first derivative DTG of the TGA curve, three clear decomposition processes are identified for McMAP: 40–190, 200–430, and 430–600 °C. The maximum temperatures of each stage are 103.4, 337.2, and 468.2 °C. The first stage of degradation corresponds to the decomposition of PVA and is attributed to the breakdown of ester bonds, the release of non-flammable gases due to the decomposition of melamine, and the evaporation of absorbed water [27,28]. The loss of mass in the second stage is caused by the elimination of  $\text{NH}_3$  from the melamine units [29]. The final stage of thermal degradation is a result of MAP decomposition in the microcapsules, which generates phosphoric acid and metaphosphoric acid, followed by their dehydration to form phosphorous oxides ( $\text{P}_4\text{O}_{10}$ ) [28,30].

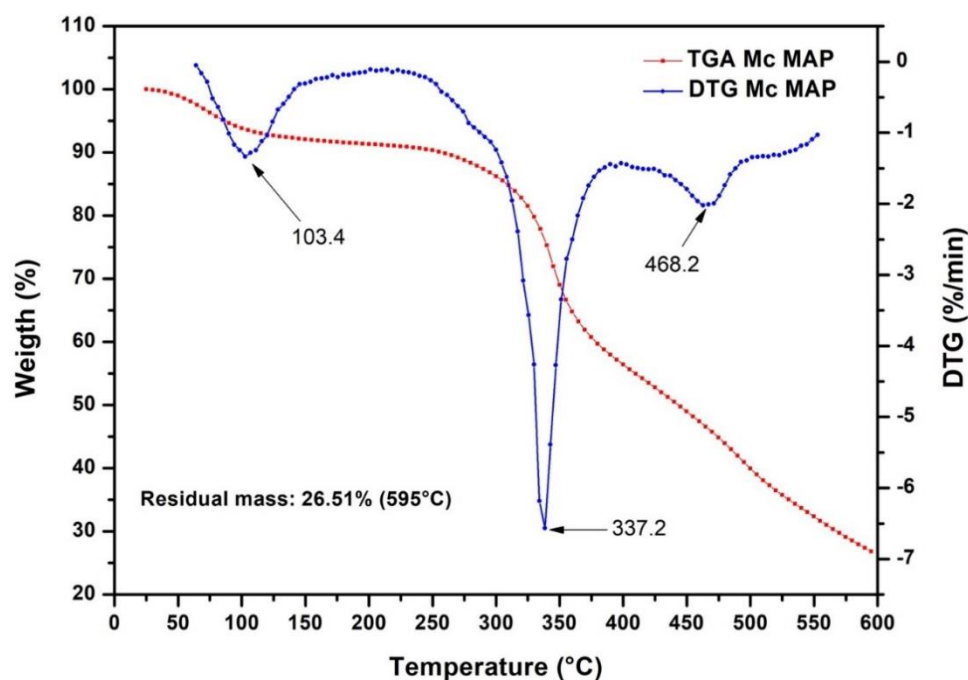


**Figure 4.** Thermogravimetric Analysis (TGA) and Differential Thermogravimetric Analysis (DTG) analysis of the McMAPs.

**Table 3.** Result of decomposition temperature and residual mass of McMAPs microcapsules.

Sample	T5%	Tmax1	Tmax2	Tmax3	Residual Mass (%)		
					400 °C	500 °C	600 °C
McMAP	90.00 °C	103.40 °C	337.20 °C	468.20 °C	50%	40%	27%

### 3.3. Formulation of Coatings with MAP Microcapsules

The particle sizes for the four formulations described in Table 1 were evaluated using the ASTM D-333 standard. For the reference formulation (F-Blank), a Hegman value of 5 (<38.10  $\mu\text{m}$ ) was determined. On the other hand, the formulations that comprised microcapsules (F-3% McMAPs and F-9% McMAPs) presented Hegman values of 4 (<50.80  $\mu\text{m}$ ). These results can be explained by the inferior dispersion of the microcapsules in suboptimal media causing agglomeration. This is the case for intumescent coating formulations that contain high solid contents, where satisfactory dispersion of the microcapsules is difficult to achieve. As previously mentioned, the formulations that include microcapsules were produced with a high-volume content of solids, exhibiting PVC contents between 49.90 and 65.42%, and a  $\lambda$  ratio in the range of 1.37 to 1.51 (Table 4). These high PVC contents produce dull coatings and inhibit blistering; however, the permeability and the risk of substrate corrosion increase. For this reason, when industrially applied on steel, these formulations must be coated with a sealant that protects it from corrosive environments. In this work, the resistance of the coatings to weathering was not evaluated and therefore a sealant was not applied.

**Table 4.** Pigment volume concentrations (PVC), critical PVC (CPVC), and  $\lambda$  values for the formulations.

Formulations	PVC	CPVC	$\lambda$
F-Blank	49.90	36.53	1.37
F-3% McMAP	58.70	39.52	1.49
F-9% McMAP	65.42	43.46	1.51

### 3.4. Evaluation of the Mechanical Properties of the Coatings

Visual inspection of the formulated coatings was conducted using opacity drawdown charts. Figure S1a–c shows the results obtained for the F-Blank and F-3% McMAP coatings. The formulations show good opacity and covering power when applied on the substrate, with slight changes in the tonality depending on the amount of inorganic filler and tannins present. These coatings form a continuous film on the substrate (Figure S1a,b), however, upon further addition of MAP microcapsules (i.e., F-9% McMAP), agglomerations and cracks were formed on the coating. Results obtained from the dynamic viscosities are shown in Table 5; when the percentage of MAP in the microcapsules increases, the viscosity increases. The F-9% McMAP sample displayed the highest viscosity with a value of 2407 cp. This is because the tannins present in the MAP microcapsules absorb any water in the formulation [11]. This high viscosity is to be expected as the coating has a high solid content, characteristic of intumescent commercial coatings. The high viscosities proved to be problematic for the application of the films onto various substrates, for this reason a brush was used.

Table 5 also shows the dry film thicknesses of the formulations on metal substrates. Figure S1d–i shows the coatings applied on a metal substrate. When two successive coatings were applied on the metallic substrate, the thicknesses of the applied coatings (F-Blank, F-3% McMAPs, and F-9% McMAPs) are between 150 and 190  $\mu\text{m}$ . Two coats of the commercial paints were also applied on the metallic substrate and these exhibited thicknesses of 256 and 49  $\mu\text{m}$  for C-INT and C-IGN, respectively. The difference in thickness is because the commercial intumescent formulation (C-INT) has a high solid content (greater than 65%). while the commercial fire-retardant paint (C-IGN) is a varnish with a solid content lower than 30%. Furthermore, the formulated and commercial coatings were

applied to wood to evaluate fire resistance properties. The thicknesses obtained for wood were lower than those applied on metal. This is most likely due to the absorption of the coating by the open pores of the medium density fiberboard (MDF) wood utilized.

**Table 5.** Evaluation of Film Properties of McMAP Formulations and Commercial Coatings.

Formulations	Viscosity (cp)	Steel Substrate	Wood Substrate	Contact Angles °
		Dry Film Thickness (μm)	Dry Film Thickness (μm)	
F-Blank	381.00	153.50 (± 15.40)	125.10 (± 0.07)	44.56 (± 1.10)
F-3% McMAP	1743.00	190.80 (± 27.40)	99.10 (± 0.49)	45.38 (± 4.78)
F-9% McMAP	2402.00	154.90 (± 13.40)	65.55 (± 2.68)	60.27 (± 6.02)
C-INT	–	256.86 (± 43.35)	65.73 (± 1.73)	43.42 (± 9.06)
C-IGN	–	49.46 (± 5.48)	61.65 (± 0.49)	70.34 (± 2.77)

Table 5 shows the contact angle results for the coatings. These results for all evaluated coatings are also shown in Figure 5. The three formulated and the two commercial coatings were hydrophilic in character, presenting contact angle values lower than 90°. The F-9% McMAP coating displayed was slightly less hydrophilic with an angle of  $60.27^\circ \pm 6.02^\circ$ . This performance is attributable to the particle sizes in the McMAPs and the roughness of the coating owing to its high solid content. As the content of microcapsules in the formulations increases, the contact angle also increases. For the F-Blank control coating, the contact angle was  $44.56^\circ \pm 1.10^\circ$ , due to the water solubility of the added tannins. Similarly, the commercial coatings present values of  $43.42^\circ$  and  $70.34^\circ$  for C-INT and C-IGN, respectively.

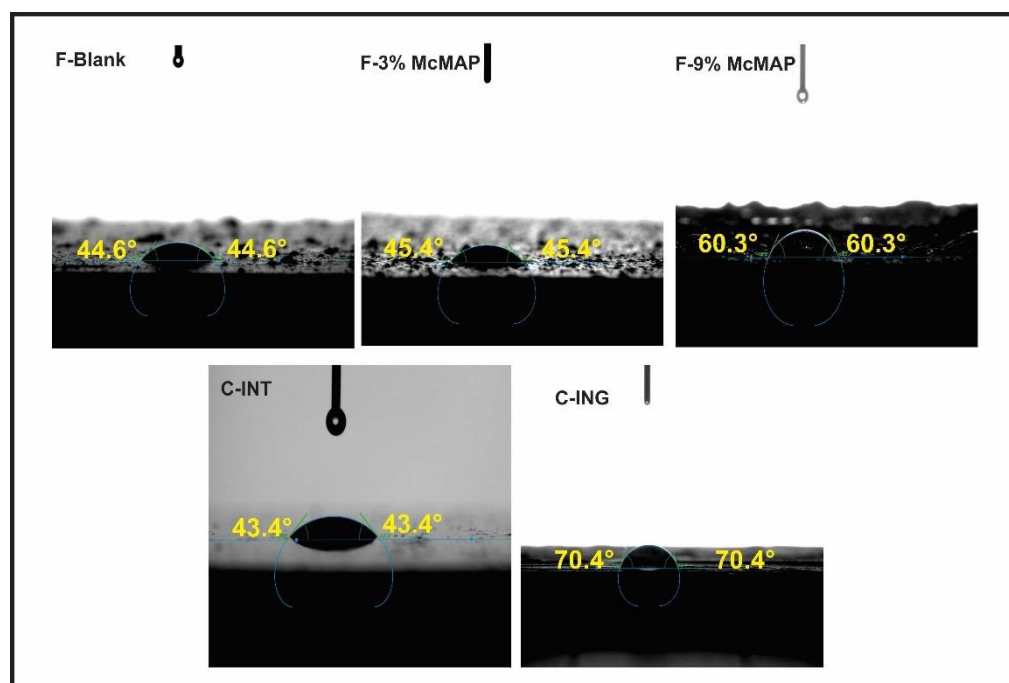


**Figure 5.** Contact angle of the formulated coatings.

Although the F-9% McMAP formulation presented the best contact angle as previously mentioned, it did not demonstrate suitable film properties. For this reason, it was not possible to determine its mechanical properties. The mechanical properties of the other coatings (formulated and commercial) were evaluated, and the results are summarized in Table 6. The 3% McMAP sample showed a slight improvement in the resistance to abrasion

with respect to the F-Blank sample and lower losses from mechanical wear were observed with a value of 179.20 mg obtained.

**Table 6.** Evaluation of the mechanical properties of coatings.

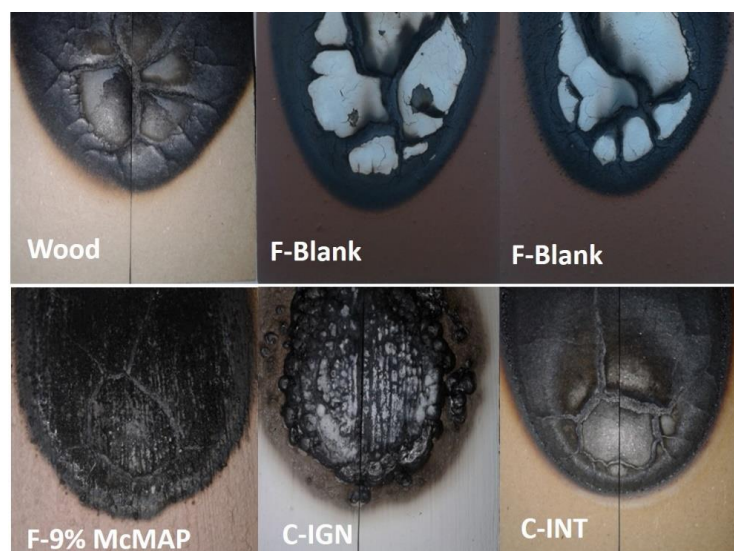
Formulations	Abrasion	Flexibility	Cupping	Adhesion	
	Wear Index (mg)	Diameter Mandrel without Fail (mm)	Impact Resistance (mm)	MPa	Type Failure
F-Blank	193.40	12	1.00 ( $\pm$ 0.68)	1.77 ( $\pm$ 0.03)	100% cohesive
F-3% McMAP	179.10	12	0.59 ( $\pm$ 0.04)	0.74 ( $\pm$ 0.04)	90% cohesive
F-9% McMAP	—	—	—	—	—
C-INT	342.70	16	1.70 ( $\pm$ 0.12)	1.06 ( $\pm$ 0.04)	90% cohesive
C-IGN	274.22	2	8.38 ( $\pm$ 0.04)	3.50 ( $\pm$ 0.69)	98% adhesive

Figure S2 shows the mass loss of the coatings for the abrasion test. The commercial coatings exhibited the greatest losses, with values of 342.70 and 274.22 mg for the C-INT and C-IGN, respectively. Flexibility tests indicated that formulated coatings performed better than the C-INT and worse than the C-ING (Figure S3). Because the latter is a varnish, it has excellent flexing properties, unlike high solid content coatings where there is a deficiency of resin in the solid volume (Table 6). The moderate behavior revealed for the F-3% McMAPs is due to the presence of McMAP particles in the formulation. These results agree with those obtained in the abrasion test. The particle size, degree of packing, and continuity of the film are determining factors for obtaining excellent mechanical film properties. A reduction in the adherence by over 50% was determined; in both formulations the failure mechanism resulted from inadequate cohesion, indicating poor physical interaction within the coating layer. Lower thickness coatings are incomparable with higher thickness coatings in terms of mechanical test.

The reference formulation (F-Blank) presented enhanced adhesion to the metallic substrate in comparison to the F-3% McMAP sample, indicating that the incorporation of the microcapsules produces a relatively negligible negative effect on the adherence to the metal.  $1.77 \pm 0.03$  MPa of adhesion was determined for F-Blank, compared to  $0.74 \pm 0.01$  MPa for F-3% McMAPs. Figure S4 shows the results of the adhesion and cupping tests. The cupping test showed similar trends to those observed in adherence tests; the commercial coatings perform better than McMAP formulated coatings. The coatings obtained with F-9% McMAPs failed to obtain film properties and covering power due to the high amount of McMAPs, for this reason, it was not possible to evaluate their mechanical properties.

### 3.5. Fire Behavior of the Coating

Fire performance tests for the formulated coatings, were performed on the wood substrate (MDF). Figure 6 shows the specimens after the flame resistance test; a zone of fire advancement was observed on the wood surface. The largest affected area and the highest fire spread rate occurred on uncoated wood, followed by F-Blank and F-9% McMAPs. For the F-3% McMAP formulation, the fire expanded to a lesser degree, behaving similarly to commercial coatings (C-INT and C-IGN). We expected that the fire-retardant effect would be superior with a higher MAP microcapsules content. However, the opposite was seen; this was attributed to the excellent properties of the 3% McMAP film where its components were homogeneously dispersed, and well-integrated with the resin. Likewise, the presence of L-MWTs and McMAPs play an important role in generating a sufficient fire-retardant effect. As such, tannins are excellent materials for generating a carbonaceous layer that prevents flame propagation. No significant intumescent behavior (foaming or swelling) was observed in any of the formulated coatings. However, a uniform carbonaceous layer was formed on the wood substrate.



**Figure 6.** Flame resistance of the formulated coatings.

Figure 7 illustrates the temperature versus time curve of the flame resistance test. This curve represents the increase in temperature of the back of the substrate, where each coating was applied. As can be seen, the flame behavior process occurs in three stages. The first stage corresponds to the initial interaction of the fire with the coating—a high-temperature gradient did not occur and it was maintained at 0–1.5 °C above the initial test temperature, whereas for C-INT,  $\Delta T = 0$  °C. In the second stage, a dramatic increase in the temperature gradient occurred from 45 to 90 s, until it reached a maximum, due to the partial loss of the coating from the substrate. The maximum obtained temperature gradients were between 10.40 and 32.80 °C. The highest gradient was obtained for F-9% McMAPs, followed by F-3% McMAPs. The final stage is the complete degradation of the coating and the advance of the fire on the wood. A decrease in  $\Delta T$  was observed due to the formation of a superficial carbonaceous layer. This effect was not seen for C-INT, in which only the first two stages were observed. This was due to the formation of foam and/or intumescence of the coating, preventing direct flame propagation and protecting the substrate.

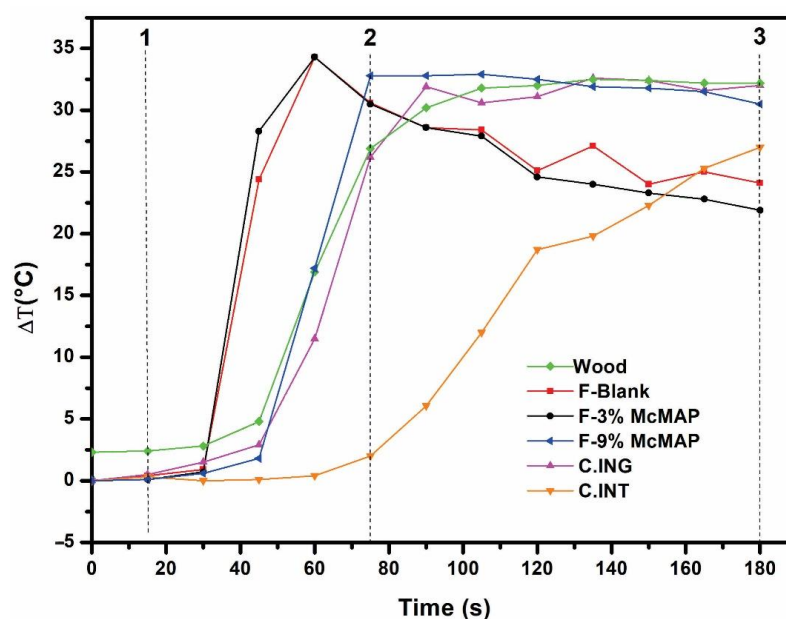


**Figure 7.** Fire behavior of the formulated coatings.

The results obtained for the carbonization index and the loss of mass in the wood substrate are reported in Table 7 and plotted in Figure 8. These tests were carried out strictly according to the ASTM D1360-90a (1994) standard methodology. The results were limited to the ASTM D1360-90a test setup, which may have been different if tested in, e.g., the ISO 5660 [31] Cone Calorimeter at varying heat fluxes or in the full-scale ISO 9705 [32] Room Corner Test—i.e., tests far outside the focus of the present study. Some materials perform well in small-scale tests but fail catastrophically in large- or full-scale situations due to high radiant heat flux levels.

**Table 7.** Mass Loss and Carbonization Index of Coatings.

Formulations	% Carbonization Index	% Mass Loss
Uncoated wood	37.40	15.80
F-Blank	33.40	11.40
F-3% McMAP	26.80	9.00
F-9% McMAP	37.80	14.30
C-INT	32.50	3.70
C-IGN	39.00	12.40

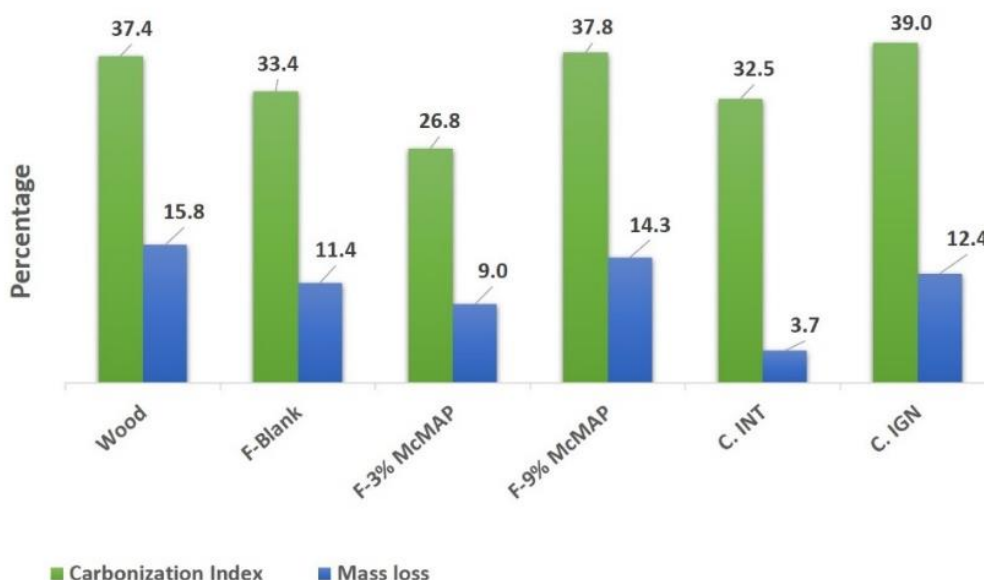


**Figure 8.** Mass loss and carbonization index of the coatings.

The best carbonization index performance was obtained for the F-3% McMAP coating with a value of 26.86%. This result confirms that superior film and mechanical properties are extremely important to enhance the fire-retardant properties. The carbonization index of uncoated wood was 37.44% indicating that coatings that contain tannins and McMAPs act as flame retardants as they generate a carbonaceous layer that reduces the mass loss of the wood substrate. The C-INT and C-IGN commercial coatings presented carbonization indices of 32.50 and 39.02%, respectively, demonstrating the superior performance of the F-3% McMAPs. Importantly, the F-3% McMAP coating displayed the lowest mass loss percentage (9.05%), better than the other formulated coatings and the uncoated wood. The mass loss of the F-3% McMAP coating is greater in comparison to the C-INT; however, its film behavior is superior. Therefore, fire-retardant properties are present in this film. On the other hand, increasing the McMAP content generates greater flame resistance; however, suitable protection was not observed since the carbonization indices and the mass loss percentage were higher. Excellent film properties are essential, as these directly influence the behavior of the coating toward fire. Noncontinuous film coatings that contain fissures or cracks allow the heat transport to pass the coating, reducing the fire resistance

properties. Although the 3% formulation was the most efficient, other studies where other percentages of microcapsules are contemplated and tests in Cone calorimetry with different heat fluxes must be carried out, for the complete characterization of the formulas and better understand their resistance against fire.

#### 4. Conclusions

We obtained MAP microcapsules through a solution-phase polymeric reaction between melamine and polyvinyl alcohol, as confirmed by FTIR and TGA. Agglomerated microspheres of uniform size were generated, with an average size of 0.98  $\mu\text{m}$  and no irregularities. The formulated coatings presented high values of PVC that increased as the incorporation of McMAPs increased, affecting the film properties. The three obtained coatings were hydrophilic in character since their contact angles were lower than 90°; however, these angles were higher than those of C-INT and were close to those of C-IGN. The mechanical properties of the F-Blank and F-3% McMAP formulated coating were similar. Increasing the amount of McMAPs did not improve the mechanical properties of the coatings; on the contrary, the properties were diminished although not significantly. The coatings containing McMAPs exhibited lower temperature gradients indicating greater resistance to fire. The fire progress and substrate temperature were well controlled by the coatings. The F-3% McMAP coating exhibited superior mechanical and fire resistance properties compared to the F-9% McMAP coating. Based on this, we conclude that the properties of the coatings deteriorate due to agglomeration upon incorporation of higher amounts of McMAPs.

**Supplementary Materials:** The following are available online at <https://www.mdpi.com/2079-6412/11/3/280/s1>, Figure S1: (a,b) Opacity tests: (a) F-Blank and (b) F-3% microcapsules of monoammonium phosphate (McMAPs); (c) F-6% McTannin; (d–g) application of the coating on metal substrate: (d) F-Blank, (e) F-3% McMAP, (f) F-6% McTannin, and (g) F-9% McMAPs. Figure S2: Wear Index F-Blank, F-3% McMAP, C.IGN and C.INT, Figure S3: Flexibility test (a) F-Blank, (b) F-3% McMAP, (c) C.IGN and (d) C.INT, Figure S4: Cupping (green bar) and Pull-off adhesion (blue bar) test on metallic substrate, Figure S5: Microencapsulation of dihydrogen ammonium phosphate (MAP) reaction without encapsulation with  $\text{Na}_2\text{CO}_3$ .

**Author Contributions:** A.D.-G. and M.E.B.: Carried out the tannin extraction and its complete characterization. J.R. and V.C.: Designed the fire-resistance and intumescence experiments. L.F.M., A.F.J., and M.E.B.: Carried out the fireproof and intumescent formulations and the dual scheme. A.M. and M.F.M.: Analyzed the results and wrote the manuscript. D.R., A.D.-G. and J.R.: Developed the field tests and consolidated the formulations obtained. All authors reviewed the manuscript and contributed to its consolidation. All authors have read and agreed to the published version of the manuscript.

**Funding:** This work was funded by ANID FONDEQUIP Project N°EQM150139, PIA/APOYO CCTE AFB170007, FONDECYT Initiation 11190358 and project FONDEF IDEA ID17i10333.

**Institutional Review Board Statement:** Not applicable.

**Informed Consent Statement:** Not applicable.

**Data Availability Statement:** Not applicable.

**Acknowledgments:** The authors would like to thank to the Interdisciplinary Group of Advanced Nanocomposites (Grupo Interdisciplinario de Nanocompuestos Avanzados, GINA) of the Department of Engineering Materials (DIMAT, according to its Spanish acronym), Engineering School of the University of Concepción, for its laboratory of nanospectroscopy (LAB-NANOSPECT). A.F.J. would like to thank the University of La Frontera. M.F.M. would like to thank Valentina Lamilla for her enormous support.

**Conflicts of Interest:** The authors declare no conflict of interest.

## References

- Jimenez, M.; Duquesne, S.; Bourbigot, S. Intumescent fire protective coating: Toward a better understanding of their mechanism of action. *Thermochim. Acta* **2006**, *449*, 16–26. [\[CrossRef\]](#)
- Puri, R.G.; Khanna, A. Effect of cenospheres on the char formation and fire protective performance of water-based intumescent coatings on structural steel. *Prog. Org. Coat.* **2016**, *92*, 8–15. [\[CrossRef\]](#)
- Han, Y.; Wu, H.; Zhang, W.; Zou, D.; Liu, G.; Qiao, G. Constitutive equation and dynamic recrystallization behavior of as-cast 254SMO super-austenitic stainless steel. *Mater. Des.* **2015**, *69*, 230–240. [\[CrossRef\]](#)
- Laoutid, F.; Bonnaud, L.; Alexandre, M.; Lopez-Cuesta, J.-M.; Dubois, P. New prospects in flame retardant polymer materials: From fundamentals to nanocomposites. *Mater. Sci. Eng. R Rep.* **2009**, *63*, 100–125. [\[CrossRef\]](#)
- Wang, Z.-Y.; Han, E.-H.; Ke, W. Fire-resistant effect of nanoclay on intumescent nanocomposite coatings. *J. Appl. Polym. Sci.* **2006**, *103*, 1681–1689. [\[CrossRef\]](#)
- Liu, Z.; Dai, M.; Zhang, Y.; Gao, X.; Zhang, Q. Preparation and performances of novel waterborne intumescent fire retardant coatings. *Prog. Org. Coat.* **2016**, *95*, 100–106. [\[CrossRef\]](#)
- Shao, Z.-B.; Deng, C.; Tan, Y.; Chen, M.-J.; Chen, L.; Wang, Y.-Z. Flame retardation of polypropylene via a novel intumescent flame retardant: Ethylenediamine-modified ammonium polyphosphate. *Polym. Degrad. Stab.* **2014**, *106*, 88–96. [\[CrossRef\]](#)
- Cao, K.; Wu, S.-L.; Wang, K.-L.; Yao, Z. Kinetic study on surface modification of ammonium polyphosphate with melamine. *Ind. Eng. Chem. Res.* **2011**, *50*, 8402–8406. [\[CrossRef\]](#)
- Liu, Z.; Dai, M.; Hu, Q.; Liu, S.; Gao, X.; Ren, F.; Zhang, Q. Effect of microencapsulated ammonium polyphosphate on the durability and fire resistance of waterborne intumescent fire-retardant coatings. *J. Coat. Technol. Res.* **2019**, *16*, 135–145. [\[CrossRef\]](#)
- Yew, M.C.; Sulong, N.R. Fire-resistive performance of intumescent flame-retardant coatings for steel. *Mater. Des.* **2012**, *34*, 719–724. [\[CrossRef\]](#)
- Wu, K.; Song, L.; Wang, Z.; Hu, Y. Microencapsulation of ammonium polyphosphate with PVA-melamine-formaldehyde resin and its flame retardance in polypropylene. *Polym. Adv. Technol.* **2008**, *19*, 1914–1921. [\[CrossRef\]](#)
- Montoya, L.; Contreras, D.; Jaramillo, A.; Carrasco, C.; Fernández, K.; Schwederski, B.; Rojas, D.; Melendrez, M. Study of anticorrosive coatings based on high and low molecular weight polyphenols extracted from the *Pine radiata* bark. *Prog. Org. Coat.* **2019**, *127*, 100–109. [\[CrossRef\]](#)
- Jaramillo, A.; Montoya, L.; Prabhakar, J.M.; Sanhueza, J.; Fernández, K.; Rohwerder, M.; Rojas, D.; Montalba, C.; Melendrez, M. Formulation of a multifunctional coating based on polyphenols extracted from the *Pine radiata* bark and functionalized zinc oxide nanoparticles: Evaluation of hydrophobic and anticorrosive properties. *Prog. Org. Coat.* **2019**, *135*, 191–204. [\[CrossRef\]](#)
- Amaral-Labat, G.; Szczurek, A.; Fierro, V.; Stein, N.; Boulanger, C.; Pizzi, A.; Celzard, A. Pore structure and electrochemical performances of tannin-based carbon cryogels. *Biomass Bioenergy* **2012**, *39*, 274–282. [\[CrossRef\]](#)
- Celzard, A.; Fierro, V.; Amaral-Labat, G.; Pizzi, A.; Torero, J. Flammability assessment of tannin-based cellular materials. *Polym. Degrad. Stab.* **2011**, *96*, 477–482. [\[CrossRef\]](#)
- ASTM D1360-90a *Standard Test Method for Small Scale Evaluation of Fire-Retardant Paints*; American Society for Testing and Materials: Philadelphia, PA, USA, 1994.
- Boccalandro, C.; Sanhueza, V.; Gómez-Caravaca, A.M.; González-Álvarez, J.; Fernández, K.; Roeckel, M.; Rodríguez-Estrada, M.T. Comparison of the composition of *Pinus radiata* bark extracts obtained at bench- and pilot-scales. *Ind. Crops Prod.* **2012**, *38*, 21–26. [\[CrossRef\]](#)
- Asbeck, W.K.; Van Loo, M. Critical pigment volume relationships. *Ind. Eng. Chem.* **1949**, *41*, 1470–1475. [\[CrossRef\]](#)
- Rodríguez, M.; Rodríguez, M.; Gracenea, J.; Saura, J.; Suay, J. The influence of the critical pigment volume concentration (CPVC) on the properties of an epoxy coating Part II. Anticorrosion and economic properties. *Prog. Org. Coat.* **2004**, *50*, 68–74. [\[CrossRef\]](#)
- ASTM D562 *Standard Test Method for Consistency of Paints Measuring Krebs Unit (KU) Viscosity Using a Stormer-Type Viscometer*; American Society for Testing and Materials: West Conshohocken, PA, USA, 2018.
- ASTM D6132-13(2017) *Standard Test Method for Nondestructive Measurement of Dry Film Thickness of Applied Organic Coatings Using an Ultrasonic Coating Thickness Gage*; American Society for Testing and Materials: West Conshohocken, PA, USA, 2017.
- ASTM D4541-17 *Standard Test Method for Pull-Off Strength of Coatings Using Portable Adhesion Testers*; American Society for Testing and Materials: West Conshohocken, PA, USA, 2017.
- ASTM D4060-19 *Standard Test Method for Abrasion Resistance of Organic Coatings by the Taber Abraser*; American Society for Testing and Materials: West Conshohocken, PA, USA, 2019.
- ISO 1519 *Paints and Varnishes—Bend Test (Cylindrical Mandrel)*; International Organization for Standardization (ISO): Geneva, Switzerland, 2011.
- ISO 1520 *Paints and Varnishes—Cupping Test*; International Organization for Standardization (ISO): Geneva, Switzerland, 2006.
- Chupin, L.; Motillon, C.; Bouhtoury, F.C.-E.; Pizzi, A.; Charrier, B. Characterisation of maritime pine (*Pinus pinaster*) bark tannins extracted under different conditions by spectroscopic methods, FTIR and HPLC. *Ind. Crops Prod.* **2013**, *49*, 897–903. [\[CrossRef\]](#)
- El-Zaher, N.A.; Osiris, W.G. Thermal and structural properties of poly(vinyl alcohol) doped with hydroxypropyl cellulose. *J. Appl. Polym. Sci.* **2005**, *96*, 1914–1923. [\[CrossRef\]](#)
- Giraud, S.; Bourbigot, S.; Rochery, M.; Vroman, I.; Tighzert, L.; Delobel, R. Microencapsulation of phosphate. *Polym. Degrad. Stab.* **2002**, *77*, 285–297. [\[CrossRef\]](#)

29. Kim, J.-H.; Kwon, D.-J.; Shin, P.-S.; Baek, Y.-M.; Park, H.-S.; Devries, K.L.; Park, J.-M. The evaluation of the interfacial and flame retardant properties of glass fiber/unsaturated polyester composites with ammonium dihydrogen phosphate. *Compos. Part B Eng.* **2019**, *167*, 221–230. [[CrossRef](#)]
30. Lim, W.P.; Mariatti, M.; Chow, W.; Mar, K. Effect of intumescent ammonium polyphosphate (APP) and melamine cyanurate (MC) on the properties of epoxy/glass fiber composites. *Compos. Part B Eng.* **2012**, *43*, 124–128. [[CrossRef](#)]
31. ISO 5660-1 Reaction-to-Fire Tests—Heat Release, Smoke Production and Mass Loss Rate—Part 1: Heat Release Rate (Cone Calorimeter Method) and Smoke Production Rate (Dynamic Measurement)); International Organization for Standardization (ISO): Geneva, Switzerland, 2015.
32. ISO 9705-1 Reaction to Fire Tests—Room Corner Test for Wall and Ceiling Lining Products—Part 1: Test Method for a Small Room Configuration; International Organization for Standardization (ISO): Geneva, Switzerland, 2016.